Electronic irradiation ageing in the vicinity of glass transition temperature for PEEK space applications

Guilhem Rival, Eric Dantras, Thierry Paulmier

Electronic irradiation ageing in the vicinity of glass transition temperature for PEEK space applications

G. Rival[a,b], E. Dantras[a,*], T. Paulmier[b],

[a] *CIRIMAT - Université Toulouse III Paul Sabatier, Physique des Polymères, 118 route de Narbonne, 31062 Toulouse, France*

[b] *ONERA - DPHY, The French Aerospace Lab, F-31055 Toulouse – France*

Abstract

Satellites in space environment are subject to several environmental constraints. In the case of polymer materials, electronic irradiations can induce premature ageing which can lead to a shorter lifetime for the satellite. Moreover, synergistic effects between temperature and irradiation can occur and enhance this ageing. A previous study showed that PolyEtherEther-Ketone (PEEK), a newly used polymer in space industry, presents great radiation tolerance properties. Nonetheless, it was necessary to investigate the influence of temperature factor on its ageing. This study focuses on the comparison of PEEK samples aged at two temperatures: room temperature and 165 °C. Irradiations have been performed under high-vacuum and with a mono-energetic electron beam. They led to doses representative of 15 years of exposure to geostationary electronic environment. The comparison between both types of samples showed that increase in irradiation temperature have a significant impact on ageing kinetics. In particular, analyses revealed a higher cross-linking density for 165 °C irradiated samples which has been associated with a higher recombination rate of radicals due to amorphous phase mobility increase above glass transition.

Keywords: Irradiation, PEEK, Structure-Properties Relationship, Temperature, Thermoplastic Polymer

*Corresponding author

Email address: eric.dantras@univ-tlse3.fr (E. Dantras)

1. Introduction

Polymers used in satellite manufacturing are exposed, in Geostationary Earth Orbit (GEO), to several environmental stresses like high-vacuum, UV and gamma radiations, thermal cycling or irradiation by high-energy particles (*e.g.* protons, electrons, ...). Thus, it is essential to understand how these different ageing factors will impact the polymer properties. In the case of electronic irradiations, two major issues can be pointed out. The first one is due to low-energy electrons which induce electrical charging of polymer surface and lead to electrostatic discharge phenomena responsible of many spacecraft failures [1]. The second one is due to high-energy electrons which depose energy in polymer volume and induce different phenomena like physico-chemical ageing [2, 3] or radiation-induced conductivity [4, 5]. Moreover, polymers have to cope with temperature variations which can induce synergistic effects with electronic irradiations. For example, an increase in the polymer temperature enhances its electrical conductivity and therefore, limits the accumulation of charges due to low-energy electrons. But also, increasing temperature can also exacerbate the radiative ageing of a polymer and significantly reduce its lifetime.

In the literature, several studies report the influence of temperature on radiative ageing [6–8]. Kudoh *et al.* showed on different polymeric materials (epoxy-based GFRP, PMMA and PTFE) that irradiation temperature has an influence on ageing even by remaining below the glass transition temperature [9]. Indeed, a decrease in irradiation temperature delays the evolution of mechanical properties due to the lowest mobility of macromolecules. In their study, Mélot *et al.* followed, by Fourier Transform InfraRed spectroscopy, the ageing of aliphatic polymers irradiated at low-temperature (*i.e.* at 8 K) [10]. Like Kudoh *et al.*, they observed a significant influence of temperature on radiative ageing but studied as well the effect of annealing after irradiation at 8 K. As a result, they showed that, even after the end of irradiation, an increase in temperature can activate the macromolecule mobility and promote the creation of new chemical bonds due to remaining radicals. Moreover, the evolution of ageing with temperature can be very non-monotonous as showed by Oshima *et al.* for PTFE [11, 12]. They observed a chain-scission phenomenon when irradiations are performed below melting temperature,

a cross-linking phenomenon just above the melting temperature and a depolymerisation phenomenon at higher temperature. However, in case of space applications, the authors did not find radiative-ageing studies which take into account the influence of the temperature factor.

This study focuses on a newly-used polymer in space industry: PolyEtherEtherKetone (PEEK). In particular, this polymer is used for structural applications in the form of PEEK / Carbon fibre composites such as in the articulated arm of the International Space Station [13] or for mechanical support applications in scientific instruments such as the search-coil magnetometer (SCM) used in the Parker Solar Probe mission [14]. In a previous study [15], PEEK has been exposed, under high-vacuum and at room temperature, to ionising electronic radiation in order to investigate its ageing behaviour for space applications. This study showed that electronic irradiations induce changes of both the amorphous phase (cross-linking) and the crystalline phase (amorphisation). In the literature, only one study tried to investigate the synergistic effects of thermal-ageing and radiative-ageing for PEEK in case of nuclear applications [16]. However, the study being focused on the comparison of thermal-ageing effect with or without irradiation, no real interpretation is made on the influence of temperature on the radiative ageing. Through this work, we propose to compare the ageing of PEEK at two irradiation temperatures chosen below and above the glass transition temperature: room temperature and 165 °C respectively. For this purpose, a heating sample-holder was developed to maintain samples at a given temperature during the irradiation. The resulting ageing has been analysed through different experimental approaches in order to probe changes at the macromolecular scale and link them to property modifications.

2. Materials and methods

2.1. Material

PEEK samples used in this study are semi-crystalline films with a thickness of 100 µm. They have been supplied by Victrex and correspond to the Aptiv 1000 grade.

2.2. Experimental simulation of electronic irradiation combined with high-temperature

In order to irradiate samples at a controlled temperature, a heating sample-holder has been developed. Figure 1 shows a schematic representation of the experimental set-up made for this purpose.

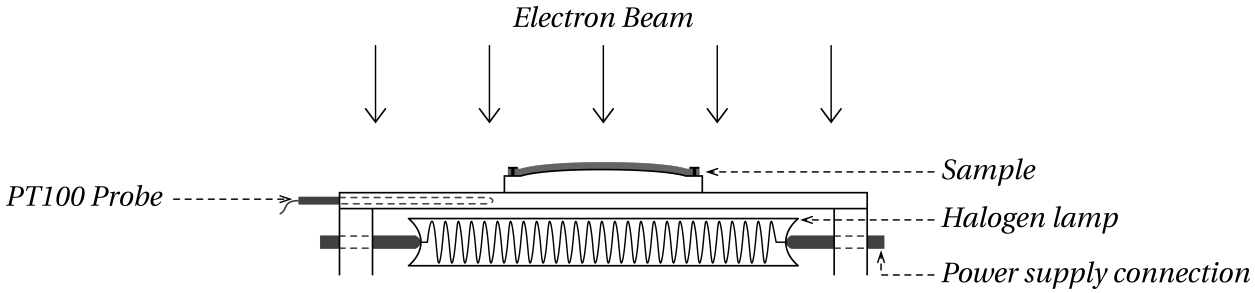

Figure 1: Schematic representation of the heating sample-holder used for irradiations at 165 °C

It consists of a 5 mm copper plate heated on the back by four halogen lamps (Reference: Orbitec R7S 400 W; 240 V) purchased from RS Components and powered by a 150 V; 3 A electrical power supply. Irradiations being performed under high-vacuum, the use of halogen lamps seemed to be the best choice for heating the sample-holder. To measure and control the temperature of the sample-holder, a PT100 sensor was coated with thermal transfer grease and inserted in the copper plate. Finally, samples were placed on curved copper plates to maximise contact with the support and are maintained at the edge by screws. Moreover, a conductive thermal transfer grease was deposited between samples and copper support to optimise heat transfer.

The procedure of irradiations at room temperature and dose calculations have been already described in a previous study [15]. In the case of irradiations at 165 °C, irradiation conditions (apart from sample temperature) and procedure are the same. They are summarised thereafter.

Irradiations were carried out in the SIRENE facility (ONERA, Toulouse, France). Samples were exposed under high-vacuum to a mono-energetic electron beam of 350 keV. Irradiations were achieved in less than 60 h thanks to a high beam current density (up to 60 nA.cm^{-2}). The resulting ionising doses D (Gy) were calculated using equation 1. All doses mentioned in this

study correspond to the average dose over the thickness of samples.

$$\mathrm{D\ (Gy = J.kg^{-1})} = 1.6\ 10^{-9} \times \Phi \frac{1}{\rho} \left(\frac{dE}{dx} \right) \tag{1}$$

Where Φ represents the total electronic fluence (electron/cm^2), ρ the material density (g.cm^{-3}) and dE/dx the electronic stopping power of the material (keV.µm^{-1}).

1.2×10^7 Gy and 3.4×10^7 Gy doses have been deposited in each type of sample (*i.e.* irradiated at room temperature and 165 °C). In these conditions, the dose profiles are homogeneous over the sample thickness (the ratio between front and back face doses is about 1.5), allowing to limit uncertainties due to a dose gradient inside samples.

2.3. Differential Scanning Calorimetry

Differential Scanning Calorimetry (DSC) analyses were performed on a DSC 7 from Perkin Elmer. Analyses were carried out under nitrogen flow and involved two heating runs and one cooling run from 50 °C to 400 °C at a rate of 10 °C.min^{-1}. The temperature of first-order transitions (*i.e.* melting temperature T_m and crystallisation temperature T_c) was taken at the maximum of the peaks and the glass transition temperature T_g was determined by the tangent method as well as the heat capacity jump ΔC_p. Crystallinity ratios χ_c were calculated from melting enthalpy using equation 2.

$$\chi_c = \frac{\Delta H_m}{\Delta H_\infty} \times 100 \tag{2}$$

Where ΔH_m is the sample melt enthalpy (J.g^{-1}), ΔH_∞ is the theoretical melt enthalpy of a fully crystalline sample reported for PEEK at 130 J.g^{-1} [17].

2.4. Acetone absorption test

Absorption tests has already proven that they can be used to study the effect of ageing on polymer materials, especially in order to probe changes in the physico-chemical structure [15]. In the case of PEEK, absorption tests were performed in acetone due to the high equilibrium

weight gain in regard of water: Stober and Seferis found a weight gain of ≈7 $\%_m$ with acetone [18] while Mensitieri *et al.* found a weight gain of ≈0.5 $\%_m$ with water [19]. Moreover, Stober and Seferis also verified that acetone penetration does not induce sample crystallisation.

The experimental procedure for weighing has already been described in our previous study [15]. We present hereafter the equation for weight gain calculations.

The weight gain (WG) is calculated by equation 3.

$$\mathrm{WG} = \frac{m - m_0}{m_0} \times 100 \tag{3}$$

Where m_0 is the initial dried mass of the sample.

Moreover, diffusion phenomena in polymer only take place in amorphous phase. Thus, the weight gain is normalised by the quantity of amorphous phase in order to consider a possible crystallinity ratio evolution. This normalised weight gain (NWG) is obtained by equation 4.

$$\mathrm{NWG} = \frac{m - m_0}{(1 - \chi_c/100) \times m_0} \times 100 \tag{4}$$

With χ_c the crystallinity ratio (%) obtained by DSC analyses.

2.5. Dynamic Mechanical Analysis

Dynamic Mechanical Analysis (DMA) tests were carried out on an ARES G2 strain-controlled rheometer from TA Instruments. Sample dimensions are 35 mm × 10.5 mm. As sample thickness does not allow a good signal-to-noise ratio in shear deformation geometry, they were analysed in tensile geometry mode. Each sample have been studied over the temperature range [–130 ; 250] °C at a rate of 3 °C.min^{-1}. Strain and frequency were fixed at 0.02 % and 1 Hz respectively allowing the determination of storage $E'_\omega(T)$ and loss $E''_\omega(T)$ moduli. For samples irradiated at room temperature, the strain used in the initial study was 0.01 %. The damping factor tan δ is then calculated by the ratio of loss modulus $E''_\omega(T)$ over storage modulus $E'_\omega(T)$.

2.6. Broadband Dielectric Spectroscopy

Broadband Dielectric Spectroscopy (BDS) is a common technique for studying dielectric behaviour of polymers and has already been extensively described [20].

Experiments were carried out on a Novocontrol BDS 4000 spectrometer associated with an Alpha-A impedance analyser. The sample diameter was 30 mm for pristine and room temperature irradiated samples, 20 mm for 165 °C irradiated samples. Analyses were performed over a frequency range of $[10^{-2}\ ;\ 10^{6}]$ Hz and for isotherms going from −150 °C to 250 °C by 5 °C steps. The complex impedance $Z^*(\omega,T)$ is used to determine the values of complex permittivity $\varepsilon^*(\omega,T)$ thanks to equation 5.

$$\varepsilon^* = \varepsilon' - i\varepsilon'' = \frac{1}{i\omega C_0 Z^*} \tag{5}$$

With $C_0 = \frac{\varepsilon_0 A}{e}$ in which ε_0 is the vacuum permittivity, A is the area of the sample and e its thickness.

Havriliak-Negami equation was used to analyse dielectric relaxation phenomena observed on loss permittivity [21, 22]:

$$\varepsilon^*(\omega) = \varepsilon_\infty + \frac{\varepsilon_s - \varepsilon_\infty}{(1 + (i\omega\tau_{HN})^{\alpha_{HN}})^{\beta_{HN}}} \tag{6}$$

ε_∞ and ε_s represent the instantaneous and the equilibrium permittivities respectively, α_{HN} and β_{HN} the Havriliak-Negami parameters which show the deviation from Debye's relaxation model (α_{HN} is related to the peak width and β_{HN} to its asymmetry at high-frequency) and τ_{HN} (s) the Havriliak - Negami relaxation time.

Sub-glass relaxations were fitted with an Arrhenius law (equation 7).

$$\tau(T) = \tau_{0,a} \exp\left(\frac{\Delta H}{RT}\right) \tag{7}$$

Where $\tau_{0,a}$ (s) is the arrhenian pre-exponential factor, ΔH (J.mol^{-1}) is the activation enthalpy of the relaxation and R the ideal gas constant.

Above glass transition, dielectric relaxations were fitted with a Vogel-Tammann-Fulcher (VTF) equation [23–25]:

$$\tau(T) = \tau_{0,v} \exp\left(\frac{1}{\alpha_f (T - T_\infty)}\right) \tag{8}$$

With $\tau_{0,v}$ (s) the vogelian pre-exponential factor, α_f (°C^{-1}) the free volume thermal expansion coefficient and T_∞ (°C) the free volume activation temperature.

3. Results and discussion

3.1. Impact of irradiation temperature on PEEK physical and chemical structures

To investigate the irradiation temperature influence on the physico-chemical structure of PEEK, DSC analyses were carried out. For purpose of clarity, DSC thermograms are not presented here. Instead, all the data extracted from these thermograms are reported in Table 1 and Figure 2 summarises the evolution of the different calorimetric parameters. Due to internal stresses which increase T_g during the first run, the T_g value presented in Figure 2 are extracted from the second runs.

This figure shows that room temperature irradiations and 165 °C irradiations induce similar evolutions of the PEEK physico-chemical structure. It means that the irradiation temperature does not affect the ageing mechanism under electronic irradiations. It is consistent with Oshima *et al.* studies on PTFE for which the degradation mechanisms only change above melting temperature [11, 12]. Nonetheless, looking at the evolutions of glass transition, melting and crystallisation temperatures, it is evident that 165 °C irradiations accelerate ageing kinetics.

- For the glass transition temperature increase, it has been previously associated with a chemical cross-linking phenomenon which occurs in the amorphous phase [15]. With increasing ageing temperature, the faster T_g increase is explained by a higher cross-link

Table 1: Data extracted from DSC analyses of samples irradiated at Room Temperature (**RT**) and irradiated at 165 °C. 1st and 2nd refers to first and second heating runs respectively.

	T_g (°C)		ΔC_p ($J.g^{-1}.°C^{-1}$)		T_m (°C)		χ_c (%)		T_c (°C)
	1st	2nd	1st	2nd	1st	2nd	1st	2nd	
Pristine	158	147	0.15	0.14	339	339	34.1	40.1	297
RT Irradiation									
Dose = 12 MGy	157	150	0.11	0.12	331	333	32.6	33.7	286
Dose = 34 MGy	159	153	0.16	0.16	318	320	25.8	23.0	269
165 °C Irradiation									
Dose = 12 MGy	158	151	0.13	0.12	327	328	30.9	30.6	280
Dose = 34 MGy	163	156	0.12	0.14	309	312	26.3	24.3	255

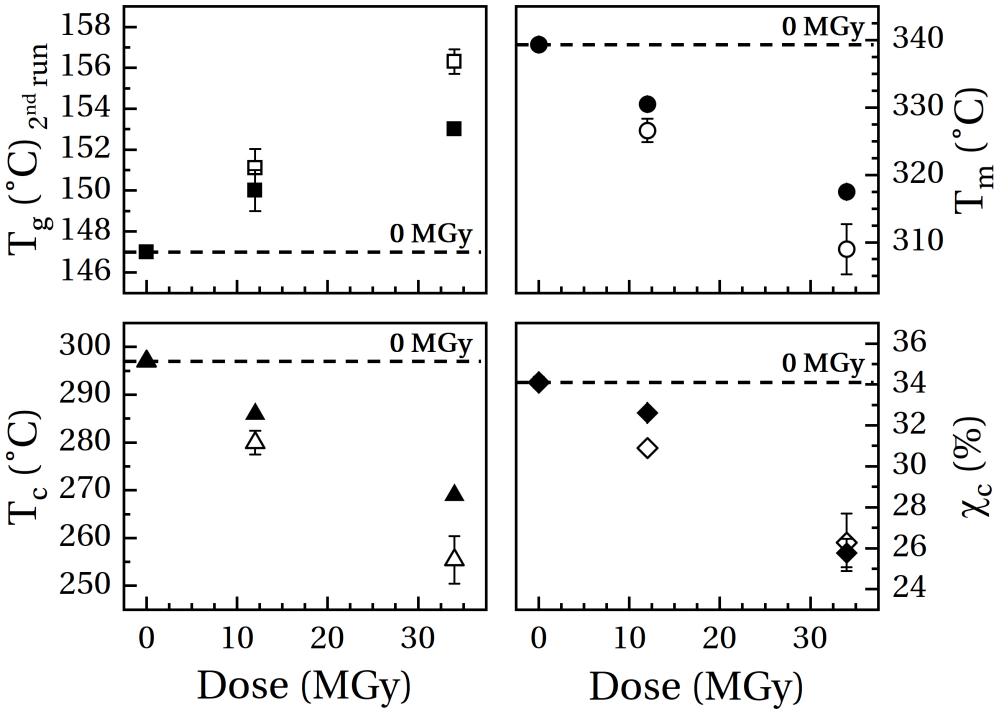

Figure 2: Calorimetric parameters extracted from DSC analyses as a function of dose. Full symbols represent room temperature irradiated samples while empty symbols represent 165 °C irradiated samples.

creation. Indeed, irradiations being performed above glass transition temperature, the higher mobility of macromolecules induces a higher recombination rate of radicals and therefore, a greater number of cross-links. By considering a three-phase model (crystalline

phase, mobile amorphous phase and rigid amorphous phase), one can calculate the mobile amorphous fraction MAF from equation 9.

$$\mathrm{MAF} = \Delta C_p / \Delta C_p^0 \tag{9}$$

Where ΔC_p^0 is the heat capacity jump of a 100 % amorphous sample reported for PEEK at 0.27 $J.g^{-1}.K^{-1}$ [26]. Finally, the rigid amorphous fraction RAF is calculated by using equation 10.

$$\mathrm{RAF} = 1 - \frac{\chi_c}{100} - \mathrm{MAF} \tag{10}$$

By using the ΔC_p value of the second heating run, the calculation of RAF gives a value of 8 % for the pristine sample, 18 % for the sample irradiated at room temperature (34 MGy), and 24 % for the sample irradiated at 165 °C (34 MGy). These results show that irradiation tends to increase the rigid amorphous fraction. The rigid amorphous phase is described as a highly entangled amorphous region where the macromolecules don't relax at the glass transition temperature. Thus, the increase in RAF can be explained by cross-links which play the role of chemical entanglements and immobilise a fraction of amorphous phase. Moreover, 165 °C irradiation induces a higher increase of the RAF which further confirms the higher cross-linking density.

The influence of this higher density of cross-linking nodes can also be seen through the sample crystallisation; *i.e.* T_c decreases faster for high-temperature irradiated samples. The higher cross-linking density further limits the crystallisability of macromolecules.

- Concerning the crystalline phase evolution, either in room temperature or in 165 °C irradiated samples, T_m and χ_c decreases are due to the creation of defects in crystallites which can be explained by a decrease in their size. This is consistent with the study of Yoda who observed by X-Ray Diffraction a 15 % decrease in the size of PEEK crystallites after electronic irradiation [27]. However, after 165 °C irradiations, only the decrease in T_m is accelerated. It means that the increase in irradiation temperature leads to less stable crystalline entities

but does not affect the crystallinity ratio. As irradiations being performed below the melting temperature, the surface of crystallites (*i.e.* at the amorphous / crystal interface) is probably mostly impacted due to the increase in amorphous phase mobility. Thus, the higher decrease in crystallite stability can be explain by a higher creation of defects mostly at their surface. However, the decrease in χ_c remains the same. During the second heating run, T_m value at a same dose remains lower for high-temperature irradiations. The samples having already melted once, these evolutions have been associated with chemical modifications. Thus, it can be associated with the higher cross-linking density which limits the crystallisation of macromolecules and leads to smaller crystallites.

3.2. Cross-linking density influence on absorption behaviour

Figure 3 shows the normalised weight gain curves for PEEK versus time square root. To emphasise the influence of irradiation temperature on the acetone absorption behaviour, only samples irradiated at 34 MGy have been studied with this method.

By representing the weight gain data as a function of time square root, a two-stage diffusion phenomenon can easily be identified for the pristine sample where the second stage, which appears at around $25\,h^{1/2}$, has a faster absorption kinetics. In the literature, Bagley and Long were the first to observe this phenomenon [28]. This two-stage mechanism is described as follow: the first part corresponds to a quasi-equilibrium which is reached at the surface of the sample and the second part to the diffusion of the penetrant through the polymer sheet which is assumed to be allowed by the rearrangement of macromolecules in the amorphous phase, *i.e.* by breaking interchain physical links. However, in this case, for which the second stage is faster than the first one, none of the previous studies provided an equation allowing to model this behaviour. For example, the study of Loh *et al.* [29] suggests a model consisting in the sum of two fickian diffusion phenomena but can't fit correctly our data.

Data show that the two studied irradiation temperatures have an opposite influence on the acetone diffusion. It can be explained by the opposite influence of amorphisation and cross-linking. While amorphisation accelerates diffusion kinetics and increases weight gain at

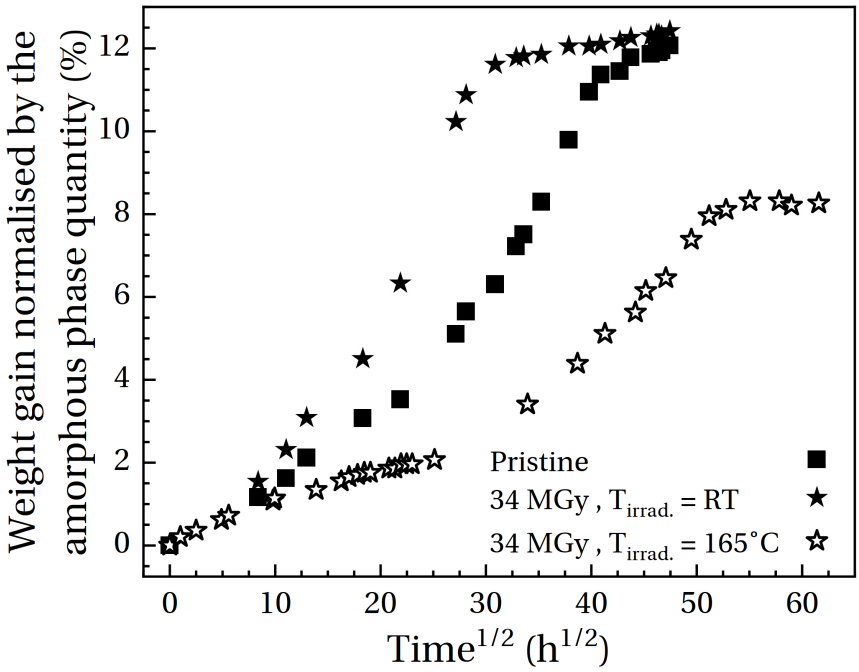

Figure 3: Weight gain data as a function of time square root for pristine PEEK and for samples irradiated at room temperature and 165 °C.

equilibrium (diffusion and retention processes taking place in amorphous phase), it has been shown that cross-linking has opposite effects [30, 31]. As already discussed in our previous study [15], the absorption behaviour of room temperature irradiated sample reveals a greater diffusion kinetics in regard to pristine sample. Therefore, the data suggest that amorphisation effects prevail over cross-linking phenomena after room temperature irradiations. However, DSC analyses presented before showed that cross-linking density is higher after irradiation at 165 °C while crystallinity ratio evolution remains similar for both irradiation conditions. Thus, the decrease in absorption kinetics and in equilibrium weight gain can be associated with the fact that cross-linking effects have become predominant over amorphisation effects.

3.3. Evolution of mechanical behaviour

Figure 4 presents the damping factor thermograms of samples irradiated at room temperature (left graph) and 165 °C (right graph).

Two mechanical relaxations can be pointed out. At low temperature, the γ relaxation is associated with localised mobility of polar groups. Studies have concluded that this relaxation is allowed by the presence of water molecules absorbed in the polymer [32, 33]. At higher temperature, the relaxation named α is associated with the mechanical manifestation of the glass transition. Mechanically, it corresponds to the transition from a glassy state to a rubbery state.

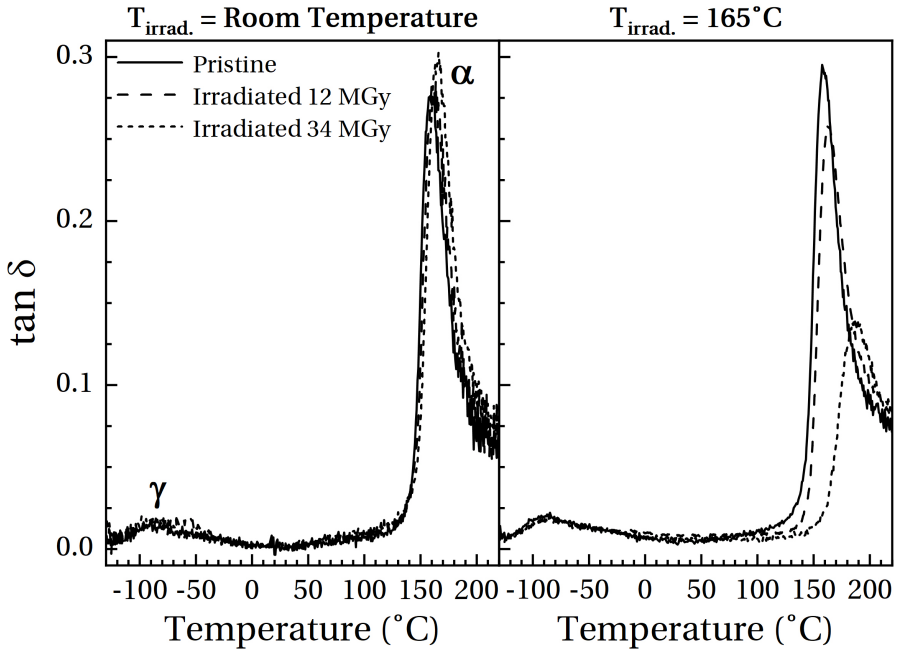

Figure 4: Damping factor thermograms of samples irradiated at room temperature and at 165 °C.

In our previous study [15], mechanical analyses showed that γ relaxation is not affected by the ageing. The cross-linking density was too low to have an effect on localised mobility. Moreover, even after irradiations at 165 °C, no evolution of this localised mobility can be observed. It indicates that the cross-linking density is not enough to modify γ mobility. NMR–^{13}C analyses were performed on pristine and 165 °C irradiated samples. No change has been observed between both NMR spectra. This result confirms the hypothesis of a low-density cross-linking. In contrast, the α relaxation is significantly modified, especially after irradiations at 165 °C. Firstly, the faster increase in T_α for high-temperature irradiated samples is the mechanical counterpart of the faster increase in T_g observed by DSC analyses.

In addition, the rubber modulus noted $\Delta E'_{220\,°C}$ ($E'_{irradiated}$-$E'_{pristine}$ at 220 °C) and α relaxation normalised area are reported in Figure 5 as a function of dose.

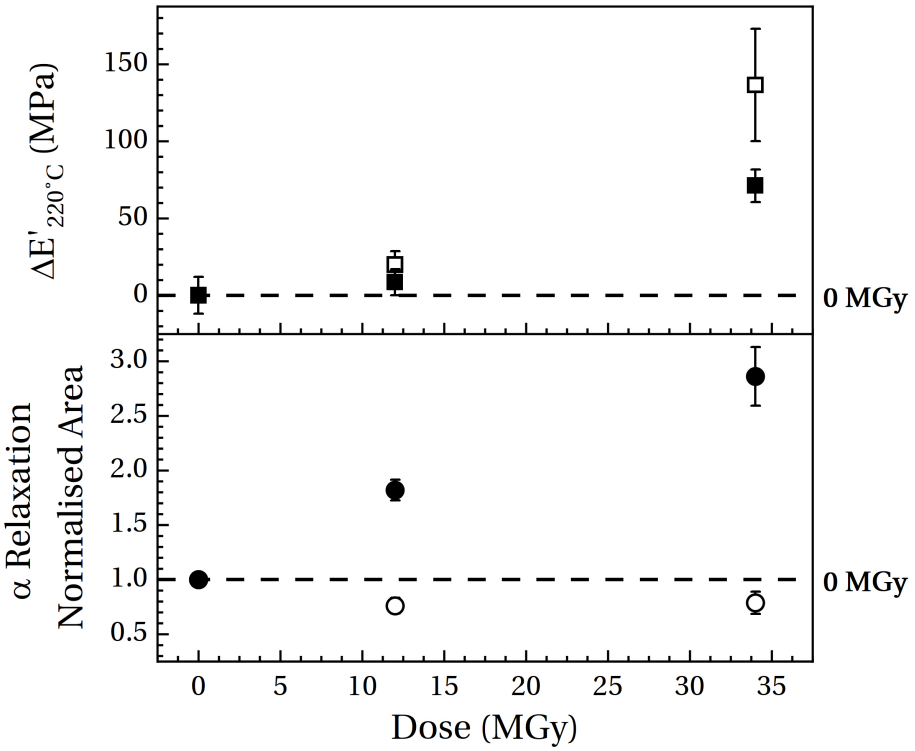

Figure 5: Rubber modulus and α relaxation normalised area as a function of dose. Full symbols represent room temperature irradiated samples while empty symbols represent 165 °C irradiated samples.

For both irradiation temperatures, the E_{rubber} value increase is directly related with the cross-link creation in the amorphous phase: cross-linking nodes limit the mobility of macromolecules and therefore, increase E_{rubber}. However, it is evident that irradiations at 165 °C induce a faster increase in E_{rubber}, despite a higher uncertainty. The equation 11 allows us to estimate an entanglement density from the rubber modulus value [34, 35].

$$\frac{1}{M_e} = \frac{1}{g'_0}\frac{E_{rubber}}{\rho RT} \tag{11}$$

Where $1/M_e$ is the density of entanglements (mol.g^{-1}), g'_0 is a factor equal to 3, E_{rubber} is the storage rubber modulus (Pa), ρ the density of PEEK (g.m^{-3}), R the ideal gas constant (J.K^{-1}.mol^{-1}) and T the temperature (K).

Thus, the evolution of entanglement density between 34 MGy irradiated samples and pristine sample give an increase of 4.6×10^{-3} mol.g^{-1} at room temperature and 7.3×10^{-3} mol.g^{-1} at 165 °C respectively. Since irradiations do not modify the ease entanglement density, this increase can only be due to cross-link density. Moreover, it shows that this increase is greater after 165 °C irradiations which confirms the hypothesis of a higher ageing kinetics with high-temperature irradiations. Nonetheless, these values need to be handled carefully and only give an estimation of the evolution of the number of entanglements / cross-links.

Finally, the normalised area, which is related to the energy dissipated by α relaxation, shows an opposite evolution between both irradiation temperatures. While a significant increase is evident after room temperature irradiations, a slight decrease is observed for samples irradiated at 165 °C. For room temperature irradiated samples, the increase in α normalised area can be linked with amorphous phase quantity increase as observed by DSC (*i.e.* decrease in χ_c). Indeed, cross-linking does not rigidify sufficiently the system in front of the mobility improve granted by the increase in amorphous quantity. For 165 °C irradiated samples, the greater cross-linking density counterbalances the effect of amorphisation and therefore, induces a decrease in energy dissipation by stiffening the amorphous phase. These conclusions are consistent with those made by studying acetone diffusion in samples and once again, show the importance of the competition between cross-linking and amorphisation.

3.4. Study of dielectric relaxations

The dielectric loss permittivity ε'' of a pristine sample is presented in Figure 6 as a function of frequency and temperature.

Three dielectric phenomena can be observed. The γ and α relaxations are consistent with relaxations observed by mechanical analyses. In addition, at low frequency and high temperature, a third dielectric phenomenon can be guessed but it is hidden by the predominance of conductivity. This last phenomenon has been associated with a Maxwell-Wagner-Sillars (MWS) polarisation [36]. It corresponds to the interfacial polarisation of crystallite induced by the difference of conductivity between crystalline and amorphous phases. In order to fit this last

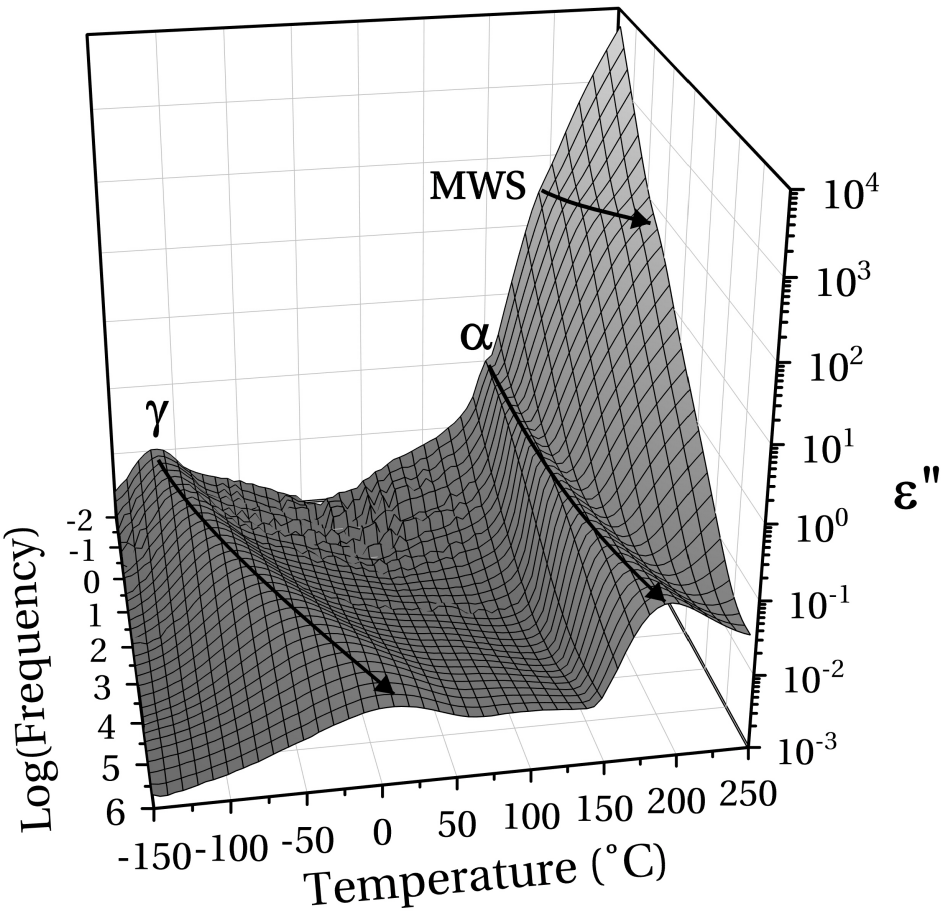

Figure 6: 3D cartography of dielectric loss permittivity ε" for the pristine sample. Arrows are intended to highlight dielectric relaxation modes.

phenomenon with equation 6, it was necessary to remove the conductivity contribution by recalculating the loss permittivity from the derivative of storage permittivity [37].

For each of these relaxation phenomena, equation 6 was used to extract the associated relaxation times. They are plotted as a function of 1000/T for each dose and irradiation temperature in the Figure 7. As expected, the sub-glass relaxation γ follows an Arrhenius behaviour while the α relaxation can be fitted with a VTF behaviour law. Curves resulting from these fits are represented in dashed lines and fit parameters are reported in Table 2. For the α relaxation, the fragility index m has been calculated with the following equation [38]:

$$m = \left(\frac{d \log(\tau)}{d (T_g/T)} \right)_{T=T_g} \tag{12}$$

In this equation, the T_g value for the second heating run is used in order to prevent the effect of internal stresses.

For the γ relaxation, the value of 49 kJ.mol^{-1} for ΔH is consistent with the literature [39, 40].

For the α relaxation, as predicted by the VTF theory, the value of $T_\infty \simeq T_g$ - 50 °C confirms its attribution to the dielectric manifestation of the glass transition. The fragility index values reported in the literature lie between 150 and 280, depending on the analysis method and on the material state [41, 42]. In this study, a value of 127 was calculated for pristine PEEK which is in the same order of magnitude as literature values.

Finally, the MWS relaxation times can be fitted by a VTF behaviour law. It indicates that this dielectric process is governed by the amorphous phase mobility.

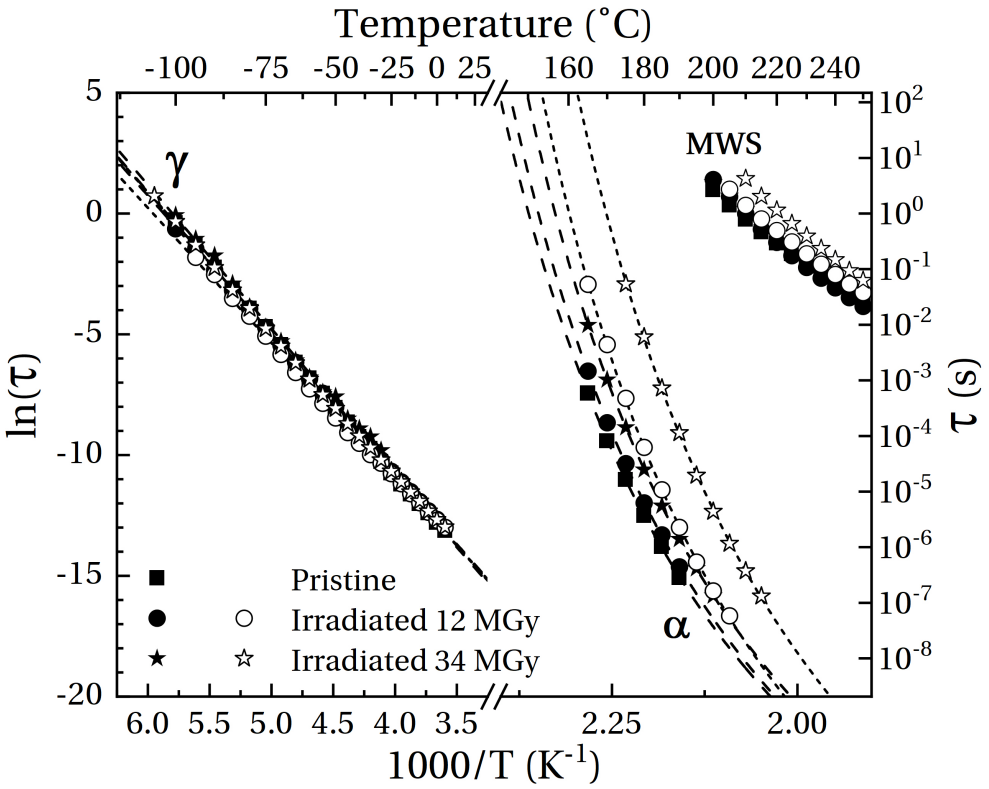

Figure 7: Arrhenius diagram of relaxation times associated with dielectric phenomena observed in PEEK samples. Full symbols represent room temperature irradiated samples while empty symbols represent 165 °C irradiated samples.

Table 2: Fit parameters obtained for dipolar relaxations and fragility indexes m of pristine, room temperature irradiated and 165°C irradiated PEEK samples.

	γ relaxation		α relaxation			
	$\tau_{0,a}$	ΔH	$\tau_{0,v}$	α_f	T_∞	m
	(s)	($kJ.mol^{-1}$)	(s)	($°C^{-1}$)	(°C)	
Pristine	1.1×10^{-15}	49.0	4.2×10^{-17}	4.42×10^{-4}	90	127
RT Irradiation						
Dose = 12 MGy	1.9×10^{-15}	48.0	4.5×10^{-17}	4.50×10^{-4}	94	128
Dose = 34 MGy	9.6×10^{-16}	49.6	6.2×10^{-17}	4.55×10^{-4}	98	133
165 °C Irradiation						
Dose = 12 MGy	3.3×10^{-15}	46.5	6.3×10^{-18}	4.12×10^{-4}	99	165
Dose = 34 MGy	1.4×10^{-15}	48.6	4.8×10^{-18}	3.69×10^{-4}	102	172

γ *relaxation*

This relaxation is not affected at all by the sample ageing, whether after room temperature irradiations or 165 °C irradiations. Like for mechanical analysis results, it indicates that the cross-linking of the amorphous phase is not sufficiently dense to modify the localised mobility response.

α *relaxation*

For this relaxation, Figure 7 shows a shift of characteristic times to higher temperatures after irradiation. Like for thermal and mechanical analyses, it indicates an increase in the thermal activation of glass transition. It is due to the cross-linking of amorphous phase which limits the macromolecule mobility. This can be view as well from the point of view of relaxation times: after irradiation, the α relaxation is shifted to longer times which is consistent with a slower relaxation kinetic. Between room temperature and 165 °C irradiations, a greater shift is observed with increasing irradiation temperature which further confirms the higher density of cross-links induced by irradiation above glass transition. This α relaxation dynamic slow-down with an increasing cross-link density has already been observed for different polymer systems [43, 44]. Moreover, Kramarenko *et al.* observed an increase in fragility index with cross-link density [44]. In this work, fragility index increases as well with ionising dose. However,

room temperature irradiated samples show a moderate increase in contrast to 165 °C irradiated samples. Therefore, this higher increase in m is consistent with a higher cross-linking density.

This shift to higher temperatures can also be noticed through the evolution of T_∞ which is represented, as well as the evolution of α_f, in Figure 8 versus ionising dose. Indeed, an increase in T_∞ value is observed with an increasing dose which is consistent with the increase in T_g observed by DSC and in T_α by DMA. These data also confirm the faster ageing induced by high-temperature irradiations with a faster increase in T_∞.

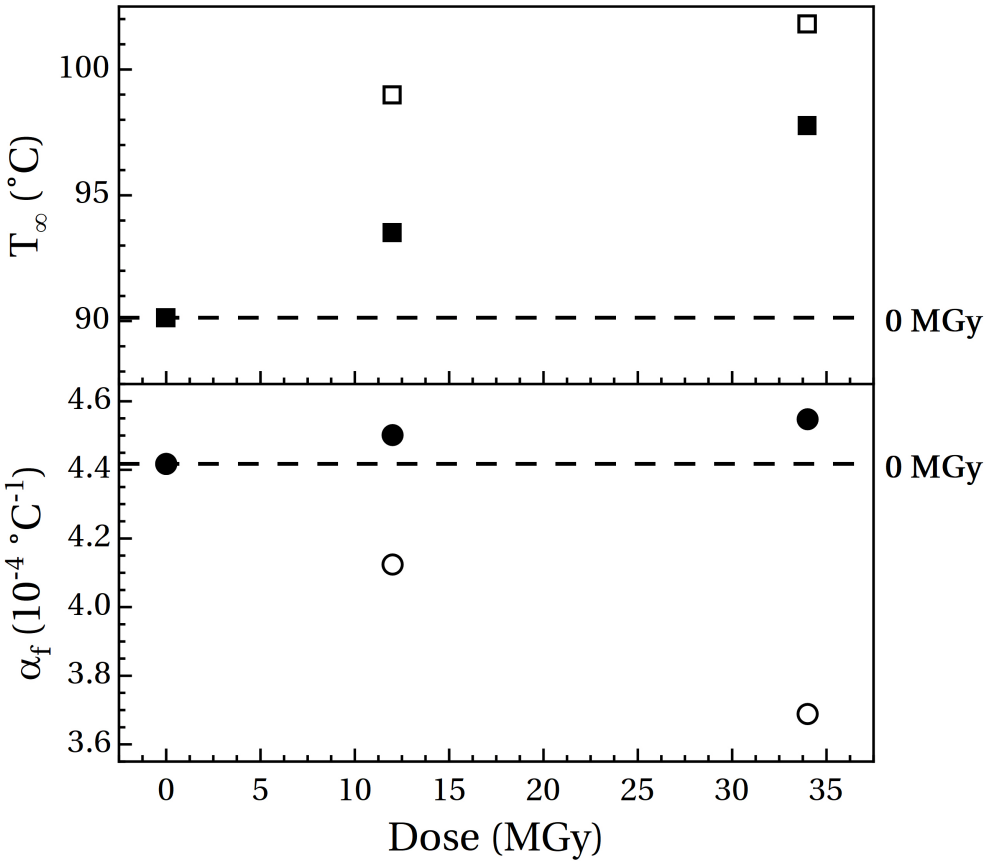

Figure 8: VTF parameters α_f and T_∞ as a function of dose for room temperature irradiated samples (full symbols) and 165 °C irradiated samples (empty symbols).

For the α_f parameter, opposite evolutions are observed between both irradiation temperatures. Like for the evolutions of diffusion kinetics and α relaxation area, these opposite tendencies can be link to the competition between amorphisation and cross-linking. For room temper-

ature irradiated samples, the slight increase in α_f is linked to the predominant influence of amorphisation. Since this parameter is associated with the free volume expansion coefficient, less crystallites induce less stresses on the amorphous phase and therefore lead to a higher expansion coefficient. Nonetheless, this effect is probably partially balanced by the cross-linking of amorphous phase which limits its mobility and consequently its possible expansion. In 165 °C irradiated samples, DSC analyses showed an equivalent amorphisation of the polymer while the density of cross-linking increases faster with ionising dose. Thus, it is assumed that the cross-linking influence becomes predominant in front of amorphisation and induces a α_f decrease.

Finally, the study of the α relaxation loss permittivity peak width can also provide information about the environment close to relaxing entities [2]. In this way, the loss permittivity peaks have been recalculated for each type of samples using the imaginary part of equation 6, which is developed in [21], and the Havriliak-Negami parameters obtained by the fit of α relaxation. This method allows us to eliminate the conductivity in order to better discern any change. The data have been normalised on position and amplitude to compare the width evolution at one isotherm and for different samples. The resulting curves, calculated at 180 °C, are represented in Figure 9 as well as the value of α_{HN} parameter which governs the peak width.

The graph shows a broadening of the α relaxation with increasing dose, either after room temperature or 165 °C irradiations. These evolutions are confirmed by the decrease in α_{HN} observed on the histogram. In the dielectric relaxation theory, this broadening is associated with an increase in the relaxation time distribution. In the case of the α relaxation, this wider distribution can be linked to a more heterogeneous environment in the vicinity of relaxing entities, *i.e.* a more heterogeneous amorphous phase. This heterogeneity increase is associated with the creation of cross-linking nodes in this phase. This figure also shows a greater heterogeneity increase for 165 °C than for room temperature irradiated samples which is the consequence of a higher cross-linking density as assumed above.

MWS relaxation

Figure 7 shows no evolution of MWS relaxation times after irradiation at room temperature but

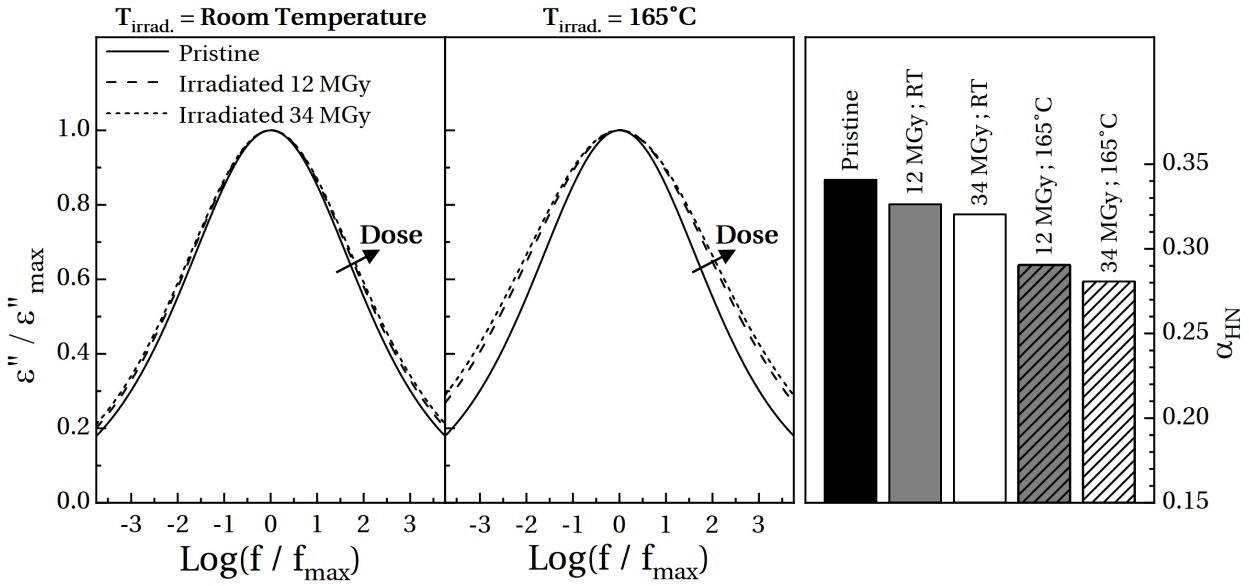

Figure 9: Normalised loss permittivity peak for α relaxation at a temperature of 180 °C (left graphs) and value of α_{HN} parameter at the same temperature (right graph).

a shift to higher temperature (longer relaxation times) once irradiated at 165 °C. It is known that the relaxation times of a MWS process is proportional to the storage permittivity ε' of the two phases (*i.e.* crystalline and amorphous) and inversely proportional to their electrical conductivity [20, p. 498]. The ε' value is dependent from the dipole density which is not modified by irradiation. Thus, the relaxation time shift can be associated with a conductivity decrease of one of them. As crystal conductivity remains stable after irradiation, this shift to longer relaxation times can indicate that irradiation at 165 °C decreases the amorphous phase conductivity. This conductivity evolution can be associated with the increase in defects (cross-links) which limits the mobility of electrical charges in the amorphous phase. For room temperature irradiated samples, this decrease is probably also present but less significant due to the lower cross-linking density. Moreover, it can be assumed that the increase in MWS relaxation times is compensated by the decrease in crystallite size, *i.e.* crystallites being smaller, their polarisation occurs at higher frequencies / shorter times.

Like for α relaxation, α_{HN} parameter can give some information on the homogeneity in the vicinity of relaxing entities. Figure 10 presents the value of this parameter at 230 °C for each sample. Crystallinity ratios obtained by DSC analyses are reported as well on the same figure.

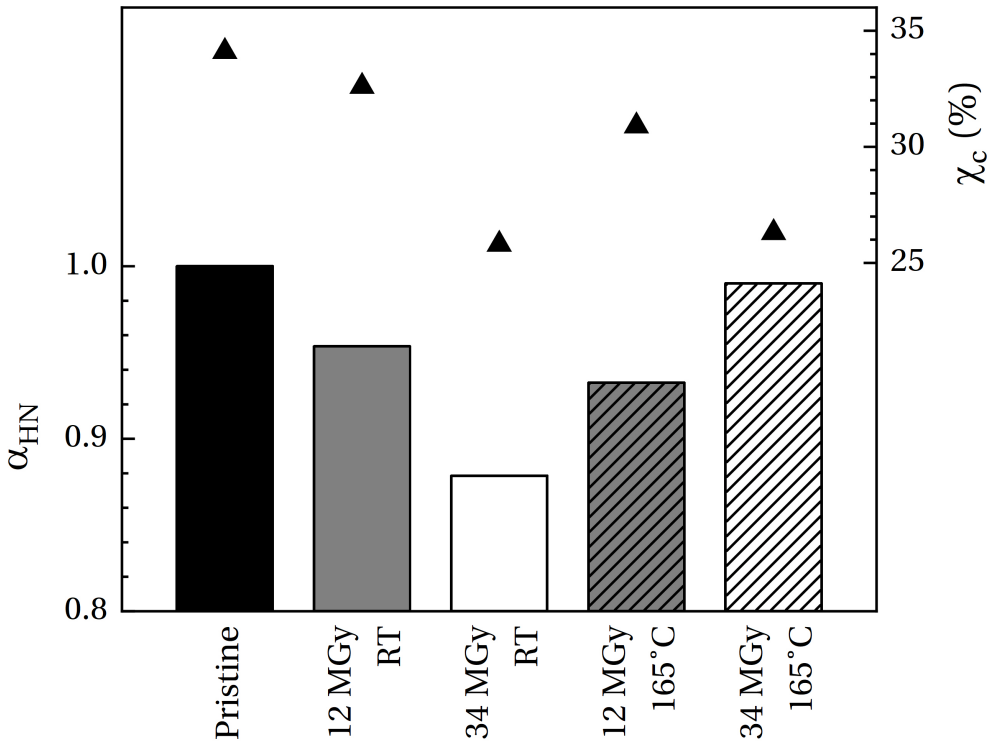

Figure 10: Value of α_{HN} parameter at 230 °C (bars) obtained for MWS mode and crystallinity ratio χ_c (symbols) obtained from DSC analyses.

For room temperature irradiated samples, the value of α_{HN} decreases with increasing ionising dose as well as the crystallinity ratio. It can be assumed that by decreasing crystallite size (associated with the decrease in T_m), irradiations also increase their size distribution and lead to a wider distribution of relaxation times. After irradiations at 165 °C, 12 MGy irradiated sample follows the same behaviour with a α_{HN} and χ_c decrease. However, for 34 MGy, the decrease in homogeneity (*i.e.* in α_{HN}) is significantly lower compared to the decrease in crystallinity ratio. It has been shown in previous studies that polymers of PolyArylEtherKetone family are subject to secondary crystallisation phenomenon; this phenomenon occurs at a temperature between glass transition and melting thanks to the higher mobility of amorphous phase [45, 46]. Thus, it can be assumed that this phenomenon promotes a reorganisation at the edge of crystallites during irradiation and leads to a crystalline phase homogenisation.

4. Conclusion

The influence of irradiation temperature on radiative ageing of PolyEtherEtherKetone by electronic irradiations has been studied. For this purpose, two irradiation campaigns have been carried out in the SIRENE facility installed at the ONERA: the first was performed at room temperature and the second at 165 °C, just above the PEEK glass transition temperature. For each irradiation temperature, two average ionising doses were deposited: 1.2×10^7 Gy and 3.4×10^7 Gy. Thanks to the high energy of electrons (350 keV), these doses are homogeneous over sample thickness.

DSC analyses showed a real influence of the temperature on the ageing kinetics. In the amorphous phase, a faster increase in T_g with dose was observed. It was associated with a higher cross-linking density due to a faster recombination rate of radicals above glass transition. In the crystalline phase, the increase in irradiation temperature only affects the evolution of T_m while the amorphisation of samples remains similar. It was associated with the fact that at 165 °C, only the mobility of amorphous phase is impacted.

These assumptions on the influence of irradiation temperature on the physico-chemical ageing were then studied and corroborated by using different probes: molecular (*i.e.* acetone diffusion), mechanical and dielectric probes.

- The higher cross-linking density in 165 °C irradiated samples has been confirmed by slower diffusion kinetics, a higher increase in rubber modulus and a shift of α relaxation times to higher temperatures. Moreover, the study of the α relaxation peak width showed that 165 °C irradiations induce a more heterogeneous medium in the vicinity of relaxing entities associated with the higher cross-linking density. Nonetheless, no evolution of γ relaxation times was observed and suggests that cross-linking density remains too low to modify localised macromolecules dynamics.
- The crystalline phase ageing was studied through the MWS relaxation. The comparison of crystallinity ratio with α_{HN} values showed that room temperature irradiations increase the heterogeneity of crystalline phase proportionally to the decrease in crystallinity ratio.

Nonetheless, maintaining samples above glass transition during 165 °C irradiations looks to homogenise crystalline phase.

- Finally, it has been shown that the competition between amorphisation and cross-linking density has a significant influence on the polymer behaviour after irradiations.

Acknowledgement

The authors would like to thank the CNES for technical support (funding of the SIRENE facility) and the Région Occitanie for financial support in this project.

References

[1] R. D. Leach, Failures and Anomalies Attributed to Spacecraft Charging, Tech. Rep. Tech. Rep. NASA-RP-1375, NASA Marshall Space Flight Center (1995).

[2] A. Roggero, E. Dantras, T. Paulmier, C. Tonon, S. Lewandowski, S. Dagras *et al.*, Dynamic glass transition of filled polysiloxane upon electron irradiation, J. Non-Cryst. Solids 455 (2017) 17–23. doi:10.1016/j.jnoncrysol.2016.10.025.

[3] A. Roggero, E. Dantras, T. Paulmier, C. Tonon, S. Dagras, S. Lewandowski *et al.*, Inorganic fillers influence on the radiation-induced ageing of a space-used silicone elastomer, Polym. Degrad. Stab. 128 (2016) 126–133. doi:10.1016/j.polymdegradstab.2016.03.010.

[4] R. Hanna, T. Paulmier, P. Molinie, M. Belhaj, B. Dirassen, D. Payan *et al.*, Radiation induced conductivity in space dielectric materials, J. Appl. Phys. 115 (2014) 033713. doi:10.1063/1.4862741.

[5] T. Paulmier, B. Dirassen, M. Belhaj, D. Rodgers, Charging Properties of Space Used Dielectric Materials, IEEE T. Plasma Sci. 43 (2015) 2894–2900. doi:10.1109/TPS.2015.2453012.

[6] J. Sun, Y. Zhang, X. Zhong, X. Zhu, Modification of polytetrafluoroethylene by radiation—1. Improvement in high temperature properties and radiation stability, Radiat. Phys. Chem. 44 (1994) 655–659. doi:10.1016/0969-806X(94)90226-7.

[7] J. Li, A. Oshima, T. Miura, M. Washio, Preparation of the crosslinked polyethersulfone films by high-temperature electron-beam irradiation, Polym. Degrad. Stab. 91 (2006) 2867–2873. doi:10.1016/j.polymdegradstab.2006.09.005.

[8] M. Ferry, E. Bessy, H. Harris, P. J. Lutz, J.-M. Ramillon, Y. Ngono-Ravache *et al.*, Aliphatic/Aromatic Systems under Irradiation: Influence of the Irradiation Temperature and of the Molecular Organization, J. Phys. Chem. B 117 (2013) 14497–14508. doi:10.1021/jp406260z.

[9] H. Kudoh, N. Kasai, T. Sasuga, T. Seguchi, Low temperature gamma-ray irradiation effects of polymer materials on mechanical property, Radiat. Phys. Chem. 43 (1994) 329–334. doi:10.1016/0969-806X(94)90021-3.

[10] M. Mélot, Y. Ngono-Ravache, E. Balanzat, Very low temperature irradiation of aliphatic polymers: Role of radical migration on the creation of stable groups (O-127), Nucl. Instrum. Meth. B 208 (2003) 345–352. doi:10.1016/S0168-583X(03)00892-9.

[11] A. Oshima, Y. Tabata, H. Kudoh, T. Seguchi, Radiation induced crosslinking of polytetrafluoroethylene, Radiat. Phys. Chem. 45 (1995) 269–273. doi:10.1016/0969-806X(94)E0009-8.

[12] Y. Tabata, A. Oshima, K. Takashika, T. Seguchi, Temperature effects on radiation induced phenomena in polymers, Radiat. Phys. Chem. 48 (1996) 563–568. doi:10.1016/0969-806X(96)00081-3.

[13] A.-M. Lanouette, M.-J. Potvin, F. Martin, D. Houle, D. Therriault, Residual mechanical properties of a carbon fibers/PEEK space robotic arm after simulated orbital debris impact, Int. J. Impact Eng. 84 (2015) 78–87. doi:10.1016/j.ijimpeng.2015.05.010.

[14] S. D. Bale, K. Goetz, P. R. Harvey, P. Turin, J. W. Bonnell, T. Dudok de Wit *et al.*, The FIELDS Instrument Suite for Solar Probe Plus: Measuring the Coronal Plasma and Magnetic Field, Plasma Waves and Turbulence, and Radio Signatures of Solar Transients, Space Sci. Rev. 204 (2016) 49–82. doi:10.1007/s11214-016-0244-5.

[15] G. Rival, T. Paulmier, E. Dantras, Influence of electronic irradiations on the chemical and structural properties of PEEK for space applications, Polym. Degrad. Stab. 168 (2019) 108943. doi:10.1016/j.polymdegradstab.2019.108943.

[16] L. Yang, Y. Ohki, N. Hirai, S. Hanada, Aging of poly(ether ether ketone) by heat and gamma rays — Its degradation mechanism and effects on mechanical, dielectric and thermal properties, Polym. Degrad. Stab. 142 (2017) 117–128. doi:10.1016/j.polymdegradstab.2017.06.002.

[17] D. J. Blundell, B. N. Osborn, The morphology of poly(aryl-ether-ether-ketone), Polymer 24 (1983) 953–958. doi:10.1016/0032-3861(83)90144-1.

[18] E. J. Stober, J. C. Seferis, Fluid sorption characterization of PEEK matrices and composites, Polym. Eng. Sci. 28 (1988) 634–639. doi:10.1002/pen.760280912.

[19] G. Mensitieri, A. Apicella, J. M. Kenny, L. Nicolais, Water sorption kinetics in poly(aryl ether ether ketone), J. Appl. Polym. Sci. 37 (1989) 381–392. doi:10.1002/app.1989.070370207.

[20] F. Kremer, A. Schönhals, Broadband Dielectric Spectroscopy, Springer, Berlin, 2003.

[21] S. Havriliak, S. Negami, A complex plane analysis of α-dispersions in some polymer systems, J. Polym. Sci. Polym. Symp. 14 (1966) 99–117. doi:10.1002/polc.5070140111.

[22] S. Havriliak, S. Negami, A complex plane representation of dielectric and mechanical relaxation processes in some polymers, Polymer 8 (1967) 161–210. doi:10.1016/0032-3861(67)90021-3.

[23] H. Vogel, The law of the relation between the viscosity of liquids and the temperature, Phys. Z. 22 (1921) 645–646.

[24] G. S. Fulcher, Analysis of recent measurements of the viscosity of glasses, J. Am. Ceram. Soc. 8 (1925) 339–355. doi:10.1111/j.1151-2916.1925.tb16731.x.

[25] G. Tammann, W. Hesse, Die Abhängigkeit der Viscosität von der Temperatur bie unterkühlten Flüssigkeiten, Z. Anorg. Allg. Chem. 156 (1926) 245–257. doi:10.1002/zaac.19261560121.

[26] S. Z. D. Cheng, M. Y. Cao, B. Wunderlich, Glass transition and melting behavior of poly(oxy-1,4-phenyleneoxy-1,4-phenylenecarbonyl-1,4-phenylene) (PEEK), Macromolecules 19 (1986) 1868–1876. doi:10.1021/ma00161a015.

[27] O. Yoda, The Crystallite Size and Lattice-Distortions in the Chain Direction of Irradiated Poly(aryl-Ether-Ketone), Polym. Commun. 26 (1985) 16–19.

[28] E. Bagley, F. A. Long, Two-stage Sorption and Desorption of Organic Vapors in Cellulose Acetate, J. Am. Chem. Soc. 77 (1955) 2172–2178. doi:10.1021/ja01613a038.

[29] W. Loh, A. Crocombe, M. Abdel Wahab, I. Ashcroft, Modelling anomalous moisture uptake, swelling and thermal characteristics of a rubber toughened epoxy adhesive, Int. J. Adhes. Adhes. 25 (2005) 1–12. doi:10.1016/j.ijadhadh.2004.02.002.

[30] L. Perrin, Q. T. Nguyen, R. Clement, J. Neel, Sorption and Diffusion of Solvent Vapours in Poly(vinylalcohol) Membranes of Different Crystallinity Degrees, Polym. Int. 39. doi:10.1002/(SICI)1097-0126(199603)39:3<251::AID-PI496>3.0.CO;2-W.

[31] K. F. Chou, S. Lee, C. C. Han, Water transport in crosslinked 2-hydroxyethyl methacrylate, Polym. Eng. Sci. 40. doi:10.1002/pen.11228.

[32] J. E. Harris, L. M. Robeson, Miscible blends of poly(aryl ether ketone)s and polyetherimides, J. Appl. Polym. Sci. 35 (1988) 1877–1891. doi:10.1002/app.1988.070350713.

[33] M. Coulson, L. Quiroga Cortés, E. Dantras, A. Lonjon, C. Lacabanne, Dynamic rheological behavior of poly(ether ketone ketone) from solid state to melt state, J. Appl. Polym. Sci. 135 (2018) 46456. doi:10.1002/app.46456.

[34] J. D. Ferry, Viscoelastic Properties of Polymers, 3rd Edition, Wiley, 1980.

[35] M. Doi, S. F. Edwards, The theory of polymer dynamics, Vol. 73, oxford university press, 1988.

[36] G. Perrier, Maxwell-Wagner-Sillars relaxations and crystallinity in PEEK, Compos. Interface. 4 (1996) 111–117. doi:10.1163/156855496X00191.

[37] M. Wübbenhorst, J. van Turnhout, Analysis of complex dielectric spectra. I. One-dimensional derivative techniques and three-dimensional modelling, J. Non-Cryst. Solids 305 (2002) 40–49. doi:10.1016/S0022-3093(02)01086-4.

[38] R. Böhmer, K. L. Ngai, C. A. Angell, D. J. Plazek, Nonexponential relaxations in strong and fragile glass formers, J. Chem. Phys. 99 (1993) 4201–4209. doi:10.1063/1.466117.

[39] M. Mourgues-Martin, A. Bernés, C. Lacabanne, Dielectric relaxation phenomena in PEEK, Thermochim. Acta 226 (1993) 7–14. doi:10.1016/0040-6031(93)80201-K.

[40] J. Audoit, L. Rivière, J. Dandurand, A. Lonjon, E. Dantras, C. Lacabanne, Thermal, mechanical and dielectric behaviour of poly(aryl ether ketone) with low melting temperature, J. Therm. Anal. Calorim. 135 (2018) 2147–2157. doi:10.1007/s10973-018-7292-x.

[41] A. G. Al Lafi, Structural development in ion-irradiated poly(ether ether ketone) as studied by dielectric relaxation spectroscopy, J. Appl. Polym. Sci. 131. doi:10.1002/app.39929.

[42] N. D. Govinna, T. Keller, C. Schick, P. Cebe, Melt-electrospinning of poly(ether ether ketone) fibers to avoid sulfonation, Polymer 171 (2019) 50–57. doi:10.1016/j.polymer.2019.03.041.

[43] J. K. W. Glatz-Reichenbach, L. Sorriero, J. J. Fitzgerald, Influence of Crosslinking on the Molecular Relaxation of an Amorphous Copolymer Near Its Glass-Transition Temperature, Macromolecules 27 (1994) 1338–1343.

[44] V. Y. Kramarenko, T. A. Ezquerra, I. Šics, F. J. Baltá-Calleja, V. P. Privalko, Influence of cross-linking on the segmental dynamics in model polymer networks, J. Chem. Phys. 113 (2000) 447–452.

[45] H. Marand, A. Prasad, On the observation of a new morphology in poly(arylene ether ether ketone). A further examination of the double endothermic behavior of poly(arylene ether ether ketone), Macromolecules 25 (1992) 1731–1736. doi:10.1021/ma00032a017.

[46] L. Quiroga Cortés, N. Caussé, E. Dantras, A. Lonjon, C. Lacabanne, Morphology and dynamical mechanical properties of poly ether ketone ketone (PEKK) with meta phenyl links, J. Appl. Polym. Sci. 133 (2016) 43396. doi:10.1002/app.43396.